Use of an ion energy analyser-mass spectrometer to measure ion kinetic-energy distributions from RF discharges in argon–helium gas mixtures

J.K. Olthoff
R.J. Van Brunt
S.B. Radovanov
J.A. Rees

Indexing terms: Ion energy analysis, Mass spectrometry, Metastable helium, Radio frequency discharges

Abstract: A mass spectrometer equipped with an electrostatic ion energy analyser has been used to measure the kinetic-energy distributions of ions sampled through an orifice in the grounded electrode of a parallel-plate radio-frequency (RF) discharge cell. Kinetic-energy distributions are presented for Ar^+, Ar_2^+, Ar^{++}, He^+, and $ArHe^+$ sampled from argon–helium plasmas with helium concentrations ranging from 0–95 mole percent, applied peak-to-peak RF voltages of 200 V, and gas pressures of 13.3 Pa. Variations in the ion kinetic-energy distributions and ion fluxes observed for different gas mixtures demonstrate the ability of this diagnostic technique to monitor plasma conditions and to investigate the ion kinetic processes occurring in the system.

1 Introduction

To understand and better utilise the possible benefits of gas mixtures in different plasma applications, such as semiconductor manufacturing, lasers, and plasma displays, it is important to identify the chemical and physical processes that play significant roles in the discharge. One possible way is by determining the identity and kinetic energy of the ions that strike the surfaces exposed to the plasma.

To develop the techniques and expertise necessary to investigate the complex and corrosive gas mixtures used in industrial applications, it is advantageous to study gas mixtures for which the fundamental ionisation, excitation and collision processes are well defined. Therefore, we have measured the kinetic-energy distributions of several ions (Ar^+, Ar_2^+, Ar^{++}, ArH^+, He^+, He_2^+, and $ArHe^+$) sampled from RF plasmas generated in gas mixtures of argon and helium. The shapes of the distributions, the relative intensities of the different ions, and the effects of changing the gas-mixture ratio provide information about the mechanisms of ion formation in the plasma, and about the properties of the plasma sheaths that are formed near surfaces exposed to the discharge. It is worth noting that the chemistry of gas mixtures, such as argon–helium, that contain metastable species is of great interest because of the role that metastable species play in the transfer of excitation energy to the other particles in the plasma [1]. The purpose of this work is to use this gas mixture to demonstrate how insight into the ion kinetics in a RF plasma can be gained from measurements of the kinetic-energy distributions of mass-identified ions.

Paper 9920A (S3), first received 5th May and in revised form 28th September 1993

J.K. Olthoff, R.J. Van Brunt and S.B. Radovanov are with the National Institute of Standards and Technology, Gaithersburg, Maryland 28099, USA

J.A. Rees is with the Department of Electrical Engineering and Electronics, The University of Liverpool, Liverpool L69 3BX, United Kingdom

2 Experiment

Radio-frequency plasmas in argon–helium mixtures were generated in a Gaseous Electronics Conference (GEC) RF reference cell [2]. Briefly, the GEC cell is a capacitively-coupled RF discharge chamber equipped with two 10.2 cm diameter parallel-plate aluminium electrodes with an interelectrode spacing of 2.54 cm. Gas is supplied to the plasma through a showerhead arrangement of small holes in the lower electrode. Mixtures of ultrahigh purity argon and helium gases are generated by controlling the flow of each gas into the cell with a mass flow controller. For the experiments presented here, the total flow was maintained at 1.7×10^{-2} Pa m^3/s (10 sccm), and the total pressure was held constant at 13.3 Pa.

The lower electrode of the GEC RF reference cell is powered through a 0.1 μF capacitor by a 13.56 MHz RF power supply, while the upper electrode is grounded to the vacuum chamber. Voltage and current waveforms are measured near the base of the powered electrode using a

The authors wish to thank S. Djurović for providing optical emission measurements of the argon–helium plasmas, and M.A. Sobolewski for his assistance in obtaining the voltage and current data. Partial support for this work was provided by the NIST Foreign Guest Scientist Program. Certain commercial equipment, instruments, or materials are identified in this paper to specify adequately the experimental procedure. Such identification does not imply recommendation or endorsement by the National Institute of Standards and Technology, nor does it imply that the materials or equipment identified are necessarily the best available for the purpose.

digital storage oscilloscope. The Fourier components of the waveforms at the surface of the powered electrode that is exposed to the plasma are then calculated using an equivalent circuit model of the RF cell [2, 3]. These calculated voltage and current amplitudes may be considered the components of the plasma voltage and current waveforms. For the discharges considered here, the applied peak-to-peak voltage (V_{RF}) measured by the oscilloscope was set at 200 V.

Ion kinetic-energy distributions (IEDs) were measured with a Hiden EQP plasma probe equipped with an electrostatic energy analyser (ESA) coupled to a quadrupole mass spectrometer (QMS). The EQP apparatus was mounted to the top of the GEC cell to allow sampling of positive ions through an 0.1 mm orifice in the grounded electrode. The IEDs are measured by setting the quadrupole to a particular mass-to-charge ratio (m/z), then scanning the energy of the ions transmitted through the ESA. All data were obtained with constant ESA/QMS settings to allow comparison of the intensities of different ion signals. The energy resolution of the ESA has been determined to be approximately 1.5 eV (full width at half maximum) for the operating conditions used here, and the uncertainty in the measured ion energies is estimated to be ± 2 eV. From independent measurements made using different electrode conditions, there is evidence that the ion signals at energies below 5 eV are subject to discrimination which affects the integrated intensities derived from the IEDs. However, the shape of the IEDs, and the trends in ion flux are reproducible under the conditions considered here. More details of the experimental apparatus and the modifications to the GEC cell required for installation of the EQP instrument are given elsewhere [4].

3 Results

Fig. 1 shows a mass spectrum of ions created in an argon–helium plasma (25% Ar, 75% He) as sampled

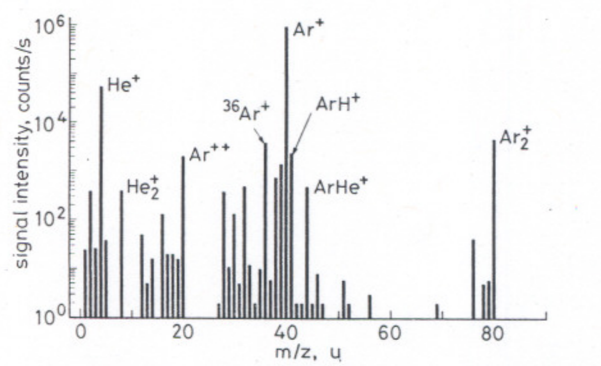

Fig. 1 *Mass spectrum of ions sampled from an argon–helium plasma in GEC RF reference cell*

Gas mixture, 25% argon and 75% helium
Pressure = 13.3 Pa, V_{RF} = 200 V, ESA was set to pass ions with kinetic energies of 20 eV

through the orifice in the grounded electrode. The ESA was set to pass only ions with kinetic energies of 20 eV. This spectrum shows which ionic species are present in the discharge, and suggests which ions should be further investigated by obtaining ion kinetic-energy distributions. The primary ions that are related to the Ar–He feed gas are labelled in Fig. 1, while the remaining peaks can be attributed to low abundance isotopes and/or plasma impurities.

The labelled peaks in Fig. 1 correspond to the ions most likely to provide information about the dominant ion processes occurring in Ar–He RF plasmas. We report IEDs of the ions Ar^+, Ar_2^+, Ar^{++}, He^+, and $ArHe^+$ for a variety of mixtures with the mole fraction of helium in the range 0–95%. An abrupt change in plasma conditions, as is evident from the optical emission and electrical characteristics, was observed when the mole fraction of helium was increased from 95% to 100%. Difficulties in obtaining IEDs were encountered in the case of pure helium, the analysis of which goes beyond the scope of this paper. The results for pure helium will be covered in a subsequent publication.

The IEDs for Ar^+ are presented in Fig. 2. For pure argon, the Ar^+ energy distribution is broadened due to

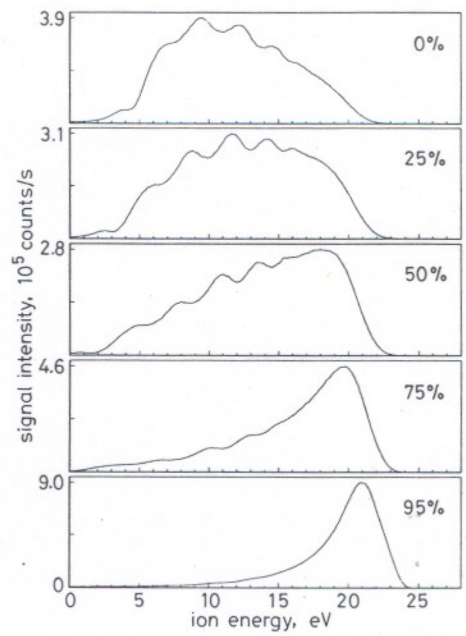

Fig. 2 *Kinetic-energy distributions (absolute ion intensity versus ion energy) of Ar^+ for RF plasmas in argon–helium mixtures at various concentrations of helium*

Total absolute pressure = 13.3 Pa, V_{RF} = 200 V
Baselines in IEDs shown in Figs. 2–6 correspond to 0 counts/s

energy loss by charge-exchange collisions and momentum transfer in elastic collisions experienced by the ions in the sheath [5]. The secondary maxima are due to the formation of thermal Ar^+ ions in the sheath by symmetric charge-exchange collisions in the presence of the RF modulated sheath potential [4–7]. As the helium concentration increases, the Ar^+ IEDs shift to higher energies with corresponding reduction in secondary maxima. This is consistent with a diminishing role played by charge transfer, and an enhanced role played by Penning ionisation in Ar^+ formation, as discussed below.

The IED for Ar_2^+ (Fig. 3) in a pure argon plasma is a narrow, featureless peak near 20 eV, consistent with ion formation in the glow region of the plasma, and minor energy losses due to collisions in the sheath. The low-intensity tail on the low-energy side of the IED results from energy loss by collisions in the sheath, while the width of the distribution is primarily determined by the time varying sheath potential. The reduction of the low-energy tail with increasing helium concentration can be accounted for by a decrease in mean-energy loss by momentum transfer resulting from an increase in relative numbers of collisions with atomic helium. The energy corresponding to the peak in the IED of Ar_2^+, approximately 20 eV, is a measure of the time-averaged plasma potential [8]. The peak energies for Ar_2^+ are observed to be relatively unaffected by the changing concentration of

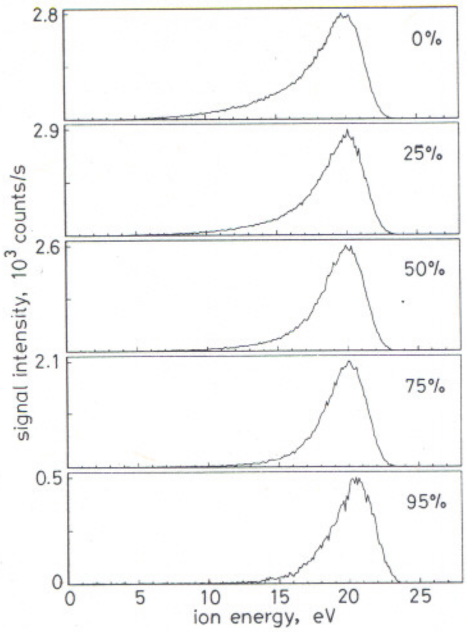

Fig. 3 *Kinetic-energy distributions (absolute ion intensity against ion energy) of Ar_2^+ for RF plasmas in argon–helium mixtures at various concentrations of helium*

Total absolute pressure = 13.3 Pa, V_{RF} = 200 V

helium in the feed gas, indicating that the plasma potential is nearly constant for all mixture ratios. The shape and trends observed for the IEDs of ArH^+ and He_2^+ were found to be similar to those of Ar_2^+, which is expected if these ions are also primarily formed in the glow region.

The shapes of the distributions for Ar^{++} (Fig. 4), are similar to those of Ar^+, except that the secondary

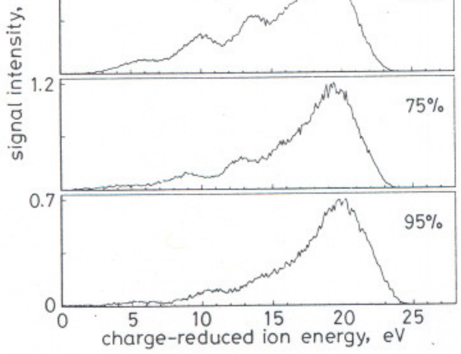

Fig. 4 *Kinetic-energy distributions (absolute ion intensity against ion energy) of Ar^{++} for RF plasmas in argon–helium mixtures at various concentrations of helium*

Total absolute pressure = 13.3 Pa, V_{RF} = 200 V

Actual kinetic energies for Ar^{++} are twice the charge-reduced energies due to the double charge present on Ar^{++}

maxima are most likely due to Ar^{++} formation in the sheath by electron-impact ionisation [4, 6]. The mean energies of the IEDs for Ar^{++} shift toward higher energies and the secondary structure diminishes in magnitude as the helium concentration increases. The energy scale in Fig. 4 corresponds to 'charge-reduced' ion energies, which means that the actual kinetic energies for Ar^{++} ions are twice those shown in the figure due to the double charge present on the ions.

Fig. 5 shows the IEDs for He^+ sampled from Ar–He plasmas with helium concentrations ranging from 25% to

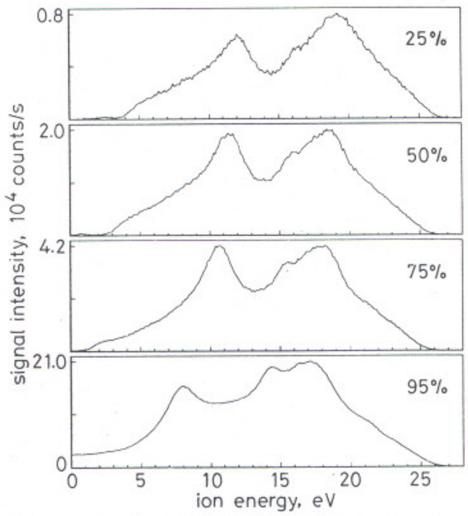

Fig. 5 *Kinetic-energy distributions (absolute ion intensity against ion energy) of He^+ for RF plasmas in argon–helium mixtures at various concentrations of helium*

Total absolute pressure = 13.3 Pa, V_{RF} = 200 V

95%. The distributions are broad, exhibit two secondary peaks, and appear to be relatively unaffected by changes in the partial pressure of helium. As for Ar^+, the He^+ distributions are broadened by collisions in the sheath, and the peaks result from formation of thermal ions by symmetric charge transfer in the time-varying sheath potential. Compared to argon, the light helium ions cross the sheath in very few RF cycles, so the He^+ distribution exhibits relatively fewer secondary peaks [7]. This also increases the effect of RF modulation on the maximum observed kinetic energy which approaches 27 eV for He^+ as compared to approximately 23 eV for Ar^+ and Ar_2^+. It should be noted that the double peak structure observed in Fig. 5 for He^+ is due to collisions in the sheath and is not related to the double-peaked or 'saddle' structure that has been observed for light ions in collisionless RF plasmas [9].

We have observed the formation of $ArHe^+$ (m/z = 44 u) in RF glow discharges in argon–helium gas mixtures with high concentrations of helium. The IEDs for ions with m/z = 44 u are shown in Fig. 6. Little signal is observed at this m/z for helium concentrations below 50%, and the majority of this signal under these conditions is undoubtedly due to CO_2^+ formation from impurities. However, as the helium concentration is increased above 75%, the detected signal at m/z = 44 u increases dramatically, indicating the formation of $ArHe^+$. The observed distribution for $ArHe^+$ at 95% helium peaks near 20 eV, like that for Ar_2^+. However, unlike for Ar_2^+, the low-energy tail in the $ArHe^+$ distribution possesses statistically significant secondary structure that is most evident for the 95% helium mixture.

Table 1 shows the magnitude and relative phases of the fundamental Fourier components of the plasma voltage and current waveforms for each gas mixture. The

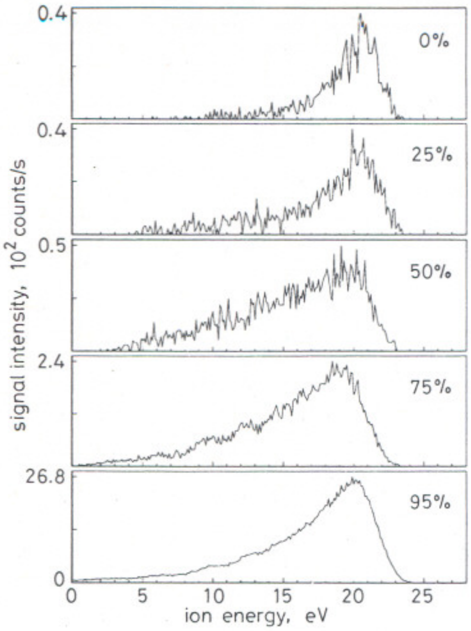

Fig. 6 *Kinetic-energy distributions (absolute ion intensity against ion energy) of $ArHe^+$ for RF plasmas in argon–helium mixtures at various concentrations of helium*

Total absolute pressure = 13.3 Pa, V_{RF} = 200 V
IEDs for partial pressures of helium of 50% and below are primarily due to the detection of CO_2^+ formed from impurities

Table 1: Amplitude of fundamental Fourier components of plasma voltage (V_1) and current (I_1) waveforms, their relative phases (ϕ_1), DC self-bias potential (V_b), and power dissipated in plasma for each of the gas mixtures utilised in experiments presented here

Helium (%)	V_1	I_1	ϕ_1	V_b	Power
	V	mA	(°)	V	W
0	122.7	228	−82.8	−90.0	1.76
25	122.8	217	−82.4	−89.4	1.77
50	122.9	202	−82.0	−89.6	1.73
75	123.2	183	−81.5	−90.3	1.67
95	123.2	158	−80.1	−91.0	1.67

Phase of I_1 is arbitrarily set to zero, and V_{RF} = 200 V for all cases

DC self-bias potential and power dissipated are also presented. Only the current and the relative phase between the current and the voltage exhibit significant dependence upon the gas mixture. The fact that V_b and V_1 are nearly independent of the gas mixture is consistent with the insensitivity of the Ar_2^+ IEDs to the gas mixture ratio (Fig. 3). These observations suggest that the plasma potential is relatively unaffected by changes in the argon–helium gas mixture ratio.

4 Discussion and conclusions

Previous information about ion formation by RF discharges in argon–helium mixtures appears to be sparse. Toups and Ernie [10] measured kinetic energy distributions for all ions (independent of mass) in a 5% argon–95% helium mixture as a function of pressure and frequency, under plasma conditions that differ from those used here. Vasile [11] measured the relative fluxes of several ions sampled from a 20% argon–80% helium plasma at 1.3 Pa using a retarding potential analyser coupled to a mass spectrometer, and compared the data to pure argon and pure helium discharges. However, they did not report energy distributions for ions from argon–helium mixtures, and did not observe all the significant ions reported here.

To understand the ion kinetic-energy distributions and the trends in ion production for argon–helium discharges, one must consider the Penning-ionisation process. The triplet metastable state of helium is thought to play a primary role in ion production because the cross-section for Penning ionisation of argon by metastable helium is higher for the triplet than for the singlet state [12], and the lifetime of the singlet state is orders of magnitude lower than the lifetime of the triplet state [13]. Additionally, investigations of afterglow [14], DC [15] and RF [16] discharges in pure helium indicate that the densities of triplet metastable helium exceed the singlet densities by more than an order of magnitude. Lawler *et al.* [15] have shown that the $He(2^3S)$ metastable state is formed primarily in the glow region because of the efficient spin conversion from the singlet-to-triplet metastable state by low-energy electrons [17]. Optical measurements in our laboratory of argon–helium RF discharges also show that the triplet helium metastable state is predominantly formed in the bulk region, and that the production rate of $He(2^3S)$ increases with increasing partial pressure of helium.

The primary processes for $He(2^3S)$ quenching in the bulk of the RF discharge are likely to be

$$He(2^3S) + Ar \rightarrow He + Ar^+ + e \qquad \text{(Penning ionisation)} \quad (1)$$

$$He(2^3S) + Ar \rightarrow ArHe^+ + e \qquad \text{(associative ionisation)} \quad (2)$$

$$He(2^3S) + He(2^3S) \rightarrow He^+ + He + e \quad (3)$$

$$e + He(2^3S) \rightarrow He^+ + 2e + h\nu \qquad \text{(collisional ionisation)} \quad (4)$$

Processes 1 and 2 are most probable for slow collisions in the thermal energy range. The destruction of triplet metastable helium and formation of He^+ by binary collisions (Reactions 3 and 4) occur predominately at higher metastable concentrations [14]. Competing processes for the de-excitation of $He(2^3S)$ that do not yield an ion include binary collisions with electrons, three-body collisions with helium atoms, and diffusion to the walls. However, these processes are slow [13] compared to reactions 1–4.

The relative importance of different processes affecting ion production in the present experiments can be assessed from the relative intensities of ions as a function of helium concentration shown in Fig. 7, which were calculated by integrating the IEDs in Figs. 2–6 over all energies. These data were derived from a set of data taken in single day, and the trends in the ion intensities were consistent with data sets obtained over several months. In agreement with Toups and Ernie [10] and Vasile [11], it is seen that Ar^+ is the dominant ion for all plasma conditions considered here. He^+ is the next most abundant ion, with an intensity that increases significantly with increasing helium concentration.

The Ar^+ flux, when normalised to the neutral argon concentration (by dividing the integrated intensity by the fractional concentration of argon), is seen to increase by more than an order of magnitude as the helium concentration in the gas mixture is increased from 0% to 95% (open circles in Fig. 7). This is consistent with an increasing contribution from Penning ionisation (reaction 1) due to increased metastable helium production. The change in shapes of the Ar^+ IEDs are also consistent with

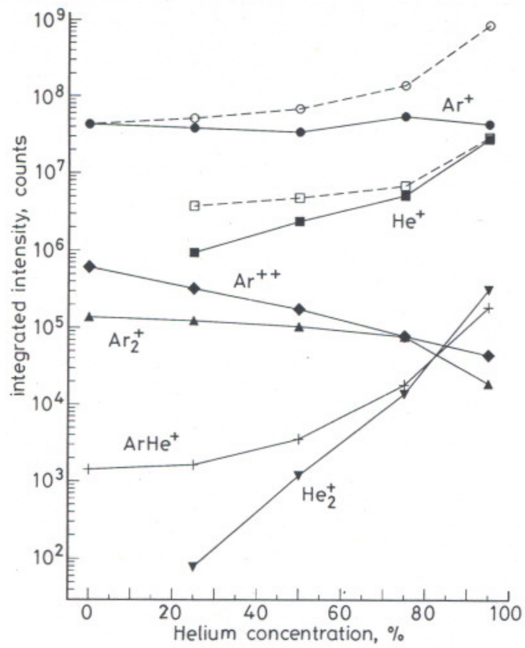

Fig. 7 *Intensity of ion signals as a function of helium concentration in feed gas*

Intensities are calculated by integrating the IEDs presented in Figs. 2–6 over all ion kinetic energies

○ Ar^+ flux normalised to concentration of neutral argon

□ He^+ flux normalised to concentration of helium

increasing Ar^+ formation by Penning ionisation. In a pure argon discharge, Ar^+ is initially formed by electron impact in the glow region. As previously noted, Ar^+ ions that experience symmetric charge-exchange in the sheath are responsible for the secondary maxima. When helium is present, the argon ions can be formed in the glow region by both electron impact and by Penning ionisation. The upward shift in Ar^+ mean energy with increasing helium content is due primarily to a decreasing contribution from symmetric charge-exchange collisions in the plasma sheath as compared to the increasing contribution from Penning ionisation in the glow. For a 95% helium mixture, the distribution peaks near 20 eV and exhibits practically no secondary structure, indicating that few Ar^+ ions are created in the sheath by symmetric charge exchange.

As the helium concentration increases, the He^+ flux goes up by more than can be explained by the increasing partial pressure of helium. This is evident in Fig. 7, where the relative He^+ signal (open squares) is plotted after being normalised for the increasing amount of helium gas present in the discharge (by dividing the integrated He^+ intensity by the fractional concentration of helium). The normalised He^+ signal increases with increasing partial pressure of helium in nearly the same manner as the normalised Ar^+ signal. This is consistent with an increasing number of He^+ ions being formed in the glow region by processes involving metastable helium, such as reactions 3 and 4. Like Ar^+, as the He^+ ions are accelerated across the sheath, they experience symmetric charge-exchange and elastic momentum-transfer collisions that lower the average ion energy and produce secondary maxima in the IED. When a sufficient number of helium atoms are present in the sheath of the discharge, symmetric charge-exchange is the dominant process influencing the observed He^+ energy distributions.

The formation of $ArHe^+$ by associative ionisation (reaction 2) is known to be a thermal process that competes with Penning ionisation. The ratio of the cross-sections for associative and Penning ionisation varies between 1% and 20% depending upon the kinetic energies of the atoms [18]. However, for the data in Fig. 7, the ratio of $ArHe^+$ to Ar^+ intensity is less than 1% under all conditions. This may be because some of the detected Ar^+ ions are also formed in the glow by electron impact, in addition to Penning ionisation. The fact that the IEDs for $ArHe^+$ (Fig. 6) are peaked near 20 eV indicate that these ions are preferentially formed in the glow region of the plasma. The $ArHe^+$ ions may also be formed by low-energy three-body collisions [19], or bimolecular collisions, such as Ar_2^+ + He, and He_2^+ + Ar. These reactions may also occur in the sheath since a substantial number of thermal Ar^+ and He^+ ions are formed by charge-transfer collisions, which would account for the small amount of structure observed in the low-energy tail of the IED for $ArHe^+$. However, the relative contribution to ions produced in the sheath from three-body collisions and associative ionisation cannot be distinguished in the measured kinetic-energy distributions.

The measured flux of He_2^+ is observed to increase by more than three orders of magnitude as the helium concentration increases from 25% to 95%. Like Ar_2^+, this ion is thought to be formed primarily in the bulk plasma by low-energy three-body collisions. The rate of formation for He_2^+ is known to be lower than for Ar_2^+ [20], in accordance with the relative ion fluxes shown in Fig. 7.

Changes in the relative ion intensities for differing gas mixtures may also be affected by corresponding changes in the kinetic-energy distributions of the electrons in the plasma. Vasile [11] has provided experimental evidence that the average electron temperature in Ar–He RF discharges increases with increasing helium concentration.

5 References

1 BEKEFI, G.: 'Principle of laser plasmas' (Wiley, New York, 1976)

2 HARGIS, P.J., GREENBERG, K.E., MILLER, P.A., GERARDO, J.B., TORCZYNSKI, J.R., RILEY, M.E., HEBNER, G.A., ROBERTS, J.R., OLTHOFF, J.K., WHETSTONE, J.R., VAN BRUNT, R.J., SOBOLEWSKI, M.A., ANDERSON, H.A., SPLICHAL, M.P., MOCK, J.L., BLETZINGER, P., GARSCADDEN, A., GOTTSCHO, R.A., SELWYN, G., DALVIE, M., HEIDENREICH, J.E., BUTTERBAUGH, J.W., BRAKE, M.L., PASSOW, M.L., PENDER, J., LUJAN, A., ELTA, M.E., GRAVES, D.B., SAWIN, H.H., KUSHNER, M.J., VERDEYEN, J.T., HORWATH, R., and TURNER, T.R.: 'The GEC rf reference cell: a defined parallel-plate radio-frequency system for experimental and theoretical studies of plasma-processing discharges', *Rev. Sci. Instrum.*, 1994, **65**, pp. 140–154

3 SOBOLEWSKI, M.A.: 'Electrical characterization of radio-frequency discharges in the gaseous electronics conference reference cell', *J. Vac. Sci. Technol. A*, 1992, **10**, pp. 3550–3562

4 OLTHOFF, J.K., VAN BRUNT, R.J., RADOVANOV, S.B., REES, J.A., and SUROWIEC, R.: 'Kinetic-energy distributions of ions sampled from argon plasmas in a parallel-plate, radio-frequency reference cell', *J. Appl. Phys.*, 1994, **75**, pp. 115–125

5 MAY, P.W., FIELD, D., and KLEMPERER, D.F.: 'Modeling radio-frequency discharges: Effects of collisions upon ion and neutral particle energy distributions', *J. Appl. Phys.*, 1992, **71**, pp. 3721–3730

6 OLTHOFF, J.K., VAN BRUNT, R.J., and RADOVANOV, S.B.: 'Ion kinetic-energy distributions in argon rf glow discharges', *J. Appl. Phys.*, 1992, **72**, pp. 4566–4574

7 WILD, C., and KOIDL, P.: 'Ion and electron dynamics in the sheath of radio-frequency glow discharges', *J. Appl. Phys.*, 1991, **69**, pp. 2909–2922

8 KOHLER, K., COBURN, J.W., HORNE, D.E., and KAY, E.: 'Plasma potentials of 13.56-MHz rf argon glow discharges in a planar system', *J. Appl. Phys.*, 1985, **57**, pp. 59–66

9 FIELD, D., KLEMPERER, D.F., MAY, P.W., and SONG, Y.P.: 'Ion energy distributions in radio-frequency discharges', *J. Appl. Phys.*, 1991, **70**, pp. 82–92

10 TOUPS, M.F., and ERNIE, D.W.: 'Pressure and frequency dependences of ion bombardment energy distributions from rf discharges', *J. Appl. Phys.*, 1990, **68**, pp. 6125–6132

11 VASILE, M.J.: 'A comparative study of the radio frequency discharge in gas mixtures of helium with fluorine, oxygen, nitrogen, and argon', *J. Appl. Phys.*, 1980, **51**, pp. 2503–2509

12 MANUS, C., PESNELLE, A., and WATEL, G.: 'Ionization by metastable atoms', *in* WATEL, G. (Ed.): 'Electronic and atomic collisions' (North-Holland, Amsterdam, 1978), pp. 525–548

13 DELCROIX, J., FERREIRA, C.M., and RICARD, A.: 'Metastable atoms and molecules in ionized gases', *in* BEKEFI, G. (Ed.): 'Principles of laser plasmas' (Wiley, New York, 1976), pp. 159–233

14 PHELPS, A.V., and MOLNAR, J.P.: 'Lifetimes of metastable states of noble gases', *Phys. Rev.*, 1953, **89**, pp. 1202–1208

15 LAWLER, J.E., DEN HARTOG, E.A., HITCHON, W.N.G., O'BRIAN, T.R., and SOMMERER, T.J.: *in* GUNDERSEN, M.A., and SCHAEFER, G. (Eds.): 'Physics and applications of pseudosparks' (Plenum Press, New York, 1989), pp. 109–132

16 GREENBERG, K.E., and HEBNER, G.A.: 'Electron and metastable densities in parallel-plate radio-frequency discharges', *J. Appl. Phys.*, 1993, **73**, pp. 8126–8133

17 PHELPS, A.V.: 'Absorption studies of helium metastable atoms and molecules', *Phys. Rev.*, 1955, **99**, pp. 1307–1313

18 NAKAMURA, H.: 'Semiempirical analysis of Penning and associative ionization of Ar in slow collisions with He(2^3S)', *Chem. Phys. Lett.*, 1978, **56**, pp. L489–L492

19 VIEHLAND, L.A., VIGGIANO, A.A., and MASON, E.A.: 'The Ar^+–He interaction potential and distribution function effects on swarm measurements of $Ar^+ + N_2$ reaction-rate coefficients using helium buffer gas', *J. Chem. Phys.*, 1991, **95**, pp. 7286–7297

20 JOHNSEN, R., CHEN, A., and BIONDI, M.A.: 'Three-body association reactions of He^+, Ne^+, and Ar^+ ions in their parent gases from 78 to 300 K', *J. Chem. Phys.*, 1980, **73**, pp. 1717–1720